



## Cationic porphyrin–quinoxaline conjugate as a photochemically triggered novel cytotoxic agent



Dalip Kumar<sup>a,\*</sup>, K. P. Chandra Shekar<sup>a</sup>, Bhupendra Mishra<sup>a</sup>, Ryohsuke Kurihara<sup>b</sup>, Maiko Ogura<sup>b</sup>, Takeo Ito<sup>b,\*</sup>

<sup>a</sup> Department of Chemistry, Birla Institute of Technology and Science, Pilani 333031, India

<sup>b</sup> Department of Energy and Hydrocarbon Chemistry, Graduate School of Engineering, Kyoto University, Kyoto 615-8510, Japan

### ARTICLE INFO

#### Article history:

Received 18 January 2013

Revised 16 March 2013

Accepted 29 March 2013

Available online 6 April 2013

#### Keywords:

Porphyrin conjugate

Quinoxaline

Photocytotoxicity

Cell viability

### ABSTRACT

A novel cationic porphyrin–quinoxaline conjugate **8** was prepared in good yield by the coupling of activated quinoxaline carboxylic acid **5** with an appropriate aminoporphyrin. The UV–vis spectra of conjugate **8** with the addition of ctDNA shows substantial hypochromicity (39%) and a red shift (12 nm) in the Soret band indicating intercalation and self stacking along the surface. The binding constant of conjugate **8** with ctDNA was determined to be  $1.26 \times 10^6 \text{ M}^{-1}$ . The porphyrin–quinoxaline conjugate **8** displayed enhanced photocytotoxicity ( $\text{IC}_{50} = 0.06 \mu\text{M}$ ) when compared to TMPyP against A549 cancer cells.

© 2013 Elsevier Ltd. All rights reserved.

Photodynamic therapy (PDT) is now an established clinical therapy for treatment of cancer.<sup>1</sup> PDT requires a combination of photosensitizer, light, and oxygen to promote the destruction of localized neoplastic lesions.<sup>2,3</sup> Though PDT is employed in most of the countries with good effect, the selectivity and side effects of commercially available PDT agents for tumor tissues offers scope for further improvement. The increase in dosage of the photosensitizer to attain the desired clinical effect lacks selectivity as well as causes tumors in sensitive areas over the body parts during the course of treatment.<sup>4</sup> The majority of reports have been focused on *meso*-tetra(4-*N*-methylpyridyl) porphyrin (TMPyP) and its metal complexes as DNA photocleaving agents studied through various spectroscopic methods. The cationic TMPyP shows a high DNA binding affinity with binding constants in the range of  $10^5$ – $10^7 \text{ M}^{-1}$  towards the negatively charged DNA strands.<sup>5–7</sup> The DNA binding mechanism is dependent on both the sequence of the DNA strands and the structure perturbation of the porphyrin molecules.<sup>8,9</sup> Additionally, the ionic strength of the solution is also known to influence the binding modes.<sup>10,11</sup> The interest in this field and the need for new molecules with improved characteristics are always high owing to diverse therapeutic applications. Several porphyrin derivatives containing delocalized positive charge substituents have been synthesized and some of these compounds were found to be efficient DNA intercalators. Porphyrins conjugated with different heterocycles such as acridine,<sup>12</sup> phenyl piper-

azine,<sup>13</sup> peptides<sup>14</sup> and natural products such as  $\beta$ -carboline<sup>15</sup> have been synthesized and evaluated for their biological properties. On the other hand, porphyrin–peptide conjugates bearing specific organelle targeting peptide sequences have also been synthesized and investigated for mitochondrial localization (MLS)<sup>16–18</sup> although the use of MLS has not yet been fully exploited as a targeting strategy for porphyrin-based sensitizers. In order to achieve the most efficient photosensitizing effect on tumor cells, the sensitizer must enter the cell and become closely associated with the subcellular structures. Photosensitizers may enter cells either directly through the plasma membrane or by endocytosis. Moreover, uptake over the plasma membrane may occur by simple or facilitated diffusion or by an active transport mechanism. The incubation parameters and mode of delivery as well as the chemical nature of the photosensitizer (molecular size, charge, water lipid partition coefficient and concentration), the type and physiological state of the cell, the environmental conditions and the nature of the carrier can all influence subcellular localization, creating a number of potential targets for photodamage.<sup>19</sup>

The quinoxaline is a useful key structural subunit in many natural and biological active molecules with various activities including anti-virus, anti-diabetic, anti-HIV, anti-fungal, anti-parasitic, anti-cancer, anti-bacterial and anti-tuberculosis.<sup>20–22</sup> The quinoxaline ring is also part of the structures in many antibiotics including actinomycin, echinomycin, lomacin and actinolite, known preventer agents for growing of gram-positive bacteria and inhibit different migratory tumors. Recently, it has been demonstrated that quinoxaline with a highly conjugated C=N bond acts as a DNA intercalating

\* Corresponding authors.

E-mail address: [dalipk@pilani.bits-pilani.ac.in](mailto:dalipk@pilani.bits-pilani.ac.in) (D. Kumar).

agent and causes light-induced DNA strand scission (500  $\mu\text{M}$ ) by generating photo-excited  $^3(n-\pi^*)$  and/or  $^3(\pi-\pi^*)$  state(s).<sup>23</sup> In our continuing design and investigation of porphyrin-based photosensitizers with improved efficacy and specific targeting properties, we report herein the synthesis of cationic porphyrin–quinoxaline conjugates **6–8** and studied their cytotoxicity and cell viability against A549 lung cancer cell line.

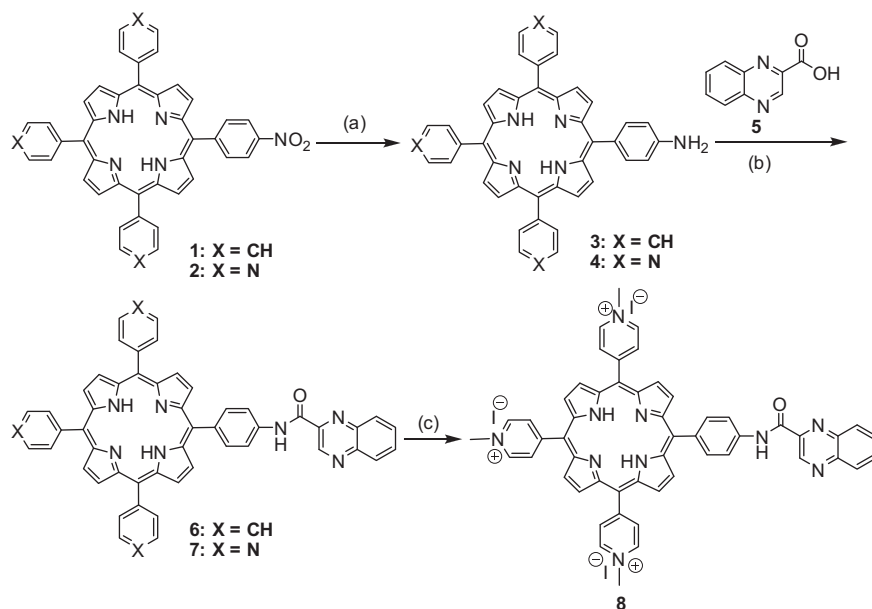
The synthesis of porphyrin–quinoxaline conjugates **6** and **8** was carried out as outlined in Scheme 1. The key intermediates triphenylporphyrinylamine **3** and tripyridylporphyrinylamine **4** were prepared using the reported protocols.<sup>24,25</sup> The nitroporphyrins **1** and **2** were reduced by using stannous chloride in 6 N HCl to afford corresponding aminoporphyrins **3** and **4** in quantitative yields. On the other hand, quinoxaline-2-carboxylic acid **5** was achieved from the reaction of *o*-phenylenediamine with *D*-fructose in acetic acid to generate tetrahydroxybutyl quinoxaline which in turn was oxidized with 30% hydrogen peroxide.<sup>26</sup> In situ activation of quinoxaline-2-carboxylic acid **5** with ethylchloroformate in presence of triethylamine followed by the addition of porphyrins **3** and **4** furnished conjugates **6** and **7** in 89% and 76% yields, respectively. The *N*-methylation of porphyrin–quinoxaline conjugate **7** with excess of methyl iodide (120 equiv) in dimethylformamide resulted in cationic porphyrin–quinoxaline conjugate **8** in 87% yield. The structures of both the conjugates were confirmed by their UV, IR, NMR ( $^1\text{H}$  and  $^{13}\text{C}$ ) and MALDI–TOF spectral data.<sup>27</sup> For cationic porphyrin **8** resonance due to *N*-methyl protons was found at  $\delta$  4.84 ppm, and internal pyrrolic NH protons were found in the up-field region at  $\delta$  –2.98 ppm. The  $^{13}\text{C}$  NMR of conjugate **8** displayed a characteristic amide carbon 162.82 ppm. The MALDI–TOF mass spectrum of cationic porphyrin–quinoxaline conjugate **8** displayed expected molecular ion peak [ $\text{M}^+$ ] at  $m/z$  833.3415.

The interactions of porphyrins **6–8** with calf thymus DNA (ctDNA) were investigated by UV–vis absorption titrations and fluorescence spectra. The spectral measurements were performed at 25  $^\circ\text{C}$  in a buffer (5 mM Tris–HCl, 0.1 M NaCl, pH 7.4). Stock solutions for porphyrins **6**, **7** and **8** were prepared in dimethyl sulfoxide. The ctDNA was procured from Merck specialties as sodium salt and its stock solutions were prepared in 0.5 mM Tris–HCl buffer and 0.1 M NaCl; dimethyl sulfoxide was less than 5% in final experimental solutions. In cationic porphyrins, the intercalative

binding is reported to occur predominantly at GC-rich regions, groove binding at AT-rich regions and outside binding at both GC-rich and AT-rich regions.<sup>28</sup> These different binding modes are distinguishable by monitoring porphyrin absorbance in the Soret region. The intercalated porphyrin species can be characterized by a large red shift of the Soret band ( $\geq 15$  nm) and a substantial hypochromicity ( $\geq 35\%$ ), whereas the groove binding results in a small red shift in the Soret band ( $\leq 8$  nm) along with little hypochromicity or hyperchromicity of the Soret maximum.<sup>29–31</sup>

The results of absorbance and emission titrations with ctDNA for porphyrin conjugate **8** are shown in Figures 1 and 2. The absorption spectra of conjugate **8** with the successive addition of ctDNA exhibited a red shift of 12 nm in the Soret region (422 nm) along with a substantial hypochromicity (39%). However, no dimerization or aggregation was observed without ctDNA in the UV spectra. As shown in Figure 2, the fluorescence spectra of conjugate **8** displayed a broad dual-band pattern in the range of 600–800 nm. The fluorescence intensities of conjugate **8** were decreased upon the addition of a small amount of ctDNA. However, further addition of ctDNA led to slightly enhanced intensity along with a small blue shift (5 nm). The spectral changes in terms of bathochromic shift and hypochromicity appeared quite similar in absorption and emission spectra. Observed spectral changes and a distinct set of isosbestic points inclined to intercalation binding.<sup>32</sup> However, initial decrease and further increase in fluorescence intensity at higher concentrations of ctDNA indicated that the porphyrin conjugate **8** adopt an intercalation binding or a combination of self-stacking with intercalation mode. Further, the corresponding association constants of porphyrin conjugates **6** ( $1.98 \times 10^5$ ) and **8** ( $1.26 \times 10^6 \text{ M}^{-1}$ ) are comparable to that of TMPyP ( $2.5 \times 10^6 \text{ M}^{-1}$ ).

The synthesized porphyrins **6**, **7** and **8** were treated with plasmid DNA (pBR322) to evaluate their DNA cleaving properties at various concentrations. The cleavage of super coiled plasmid DNA was determined quantitatively by the effective conversion of super coiled form (form I) to nicked circular form (form II) as shown in Figures 3 and 4 at different porphyrin concentrations. Surprisingly, porphyrin **6** showed complete cleavage at 50  $\mu\text{M}$  concentration in UV irradiation at a time interval of 30 and 60 min, whereas no phenomenal cleavage was observed in presence of visible light



**Scheme 1.** Reagents and conditions: (a)  $\text{SnCl}_2 \cdot 2\text{H}_2\text{O}$ , 6 N HCl (70%); (b) ClCOOEt, TEA, DCM (76%); (c)  $\text{CH}_3\text{I}$ , DMF (87%).

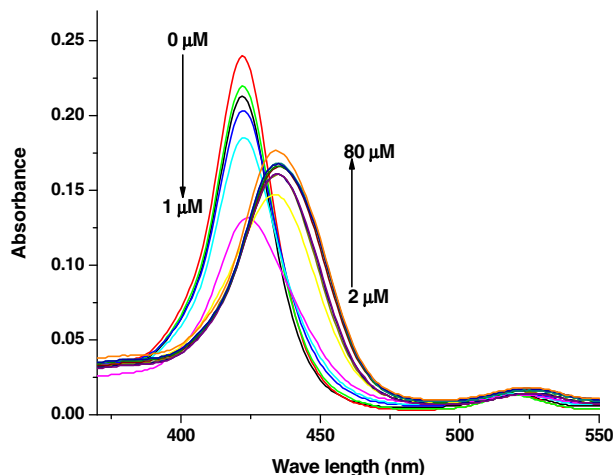


**Figure 1.** Absorption spectra of porphyrin **8**. [Porphyrin] = 2 μM, in 0.5 M Tris–HCl buffer, 0.1 M NaCl, pH –7.4. (↓, ↑) Arrow indicate the change in intensity with increase in ctDNA concentrations.

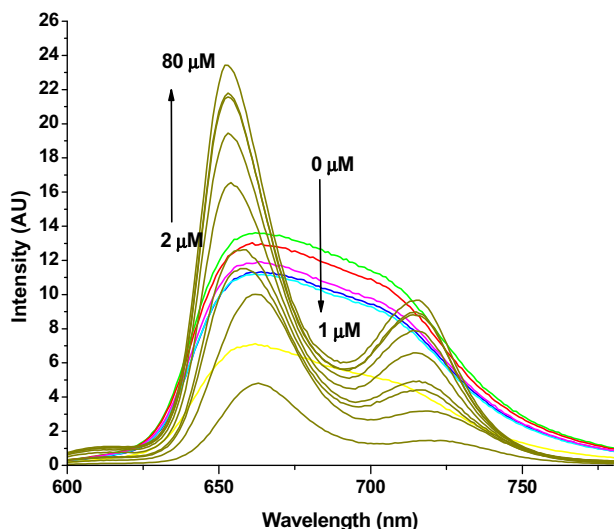


**Figure 2.** Fluorescence spectra of porphyrin **8**. [Porphyrin] = 2 μM, in 0.5 M Tris–HCl buffer, 0.1 M NaCl, pH –7.4. (↓, ↑) Arrow indicate the change in intensity with increase in ctDNA concentrations. ( $\lambda_{exc}$  –422 nm).

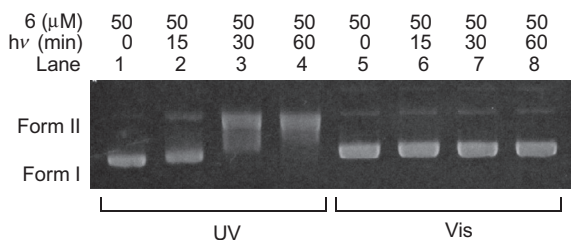


**Figure 3.** Photoinduced DNA cleavage by **6**. pBR322 supercoiled DNA (0.5 μg) was incubated with **6** (50 μM) in 20 μl of Tris–HCl (20 mM, pH 7.6) containing NaCl (20 mM) and DMSO (5 vol %) at ambient temperature in the dark for 30 min, and exposed to either UV (310–390 nm) or visible-light (>400 nm) for 0–60 min. The samples were analyzed by 1% agarose gel electrophoresis. Lanes 1–4, UV-irradiated; lanes 5–8, visible-light-irradiated.

(Figure 3). The cleavage in UV irradiation was expected due to the presence of quinoxalinein porphyrin **6**.<sup>23</sup> Moreover, porphyrin–quinoxaline conjugate **8** showed only moderate cleavage in UV as well as in visible light (Figure 4).

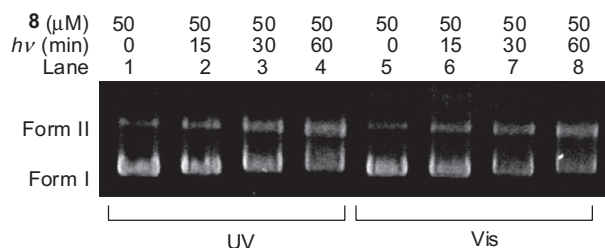


**Figure 4.** Photoinduced DNA cleavage by **8**. pBR322 supercoiled DNA (0.5 μg) was incubated with **8** (50 μM) in 20 μl of Tris–HCl (20 mM, pH 7.6) containing NaCl (20 mM) and DMSO (5 vol %) at ambient temperature in the dark for 30 min, and exposed to either UV (310–390 nm) or visible-light (>400 nm) for 0–60 min. The samples were analyzed by 1% agarose gel electrophoresis. Lanes 1–4, UV-irradiated; lanes 5–8, visible-light-irradiated.

To verify the phototoxic effects of porphyrins **6**, **7** and **8** towards A549 lung carcinoma cells, we evaluated cell viability by using the WST method. A549 cells were incubated with the porphyrins for 24 h at 37 °C, washed with PBS and then exposed to UV as well as visible light for 10 min. Further, they were incubated for 24 h and their cell viability was determined (Figure 5). Cytotoxicity was expressed as IC<sub>50</sub> values as shown in Table 1.

Comparing the effects of porphyrin **8** in the tumor cell line with TMPyP under visible light (see Supplementary data), it was found that porphyrin **8** has shown lower IC<sub>50</sub> value of 60 nM, whereas

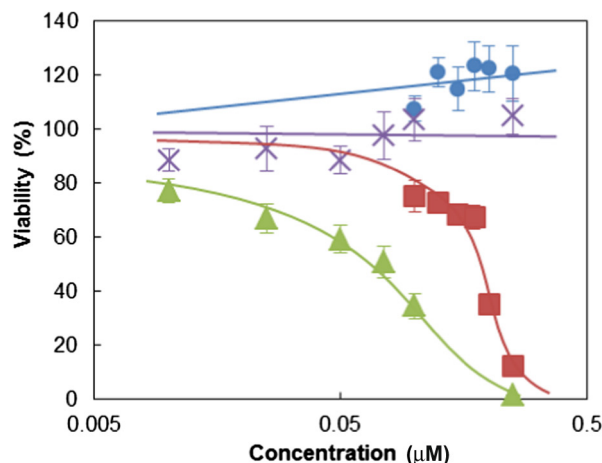
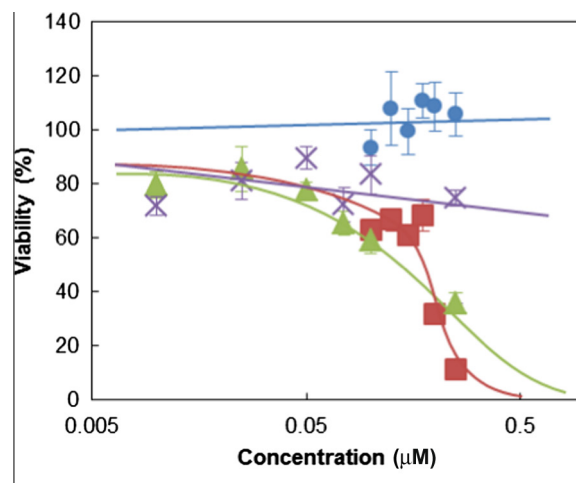


**Figure 5.** Viability of A549 lung cancer cells incubated with various concentrations of (●) **6**, (■) **7**, (▲) **8** and (×) H<sub>2</sub>TPP after (upper) UV light irradiation (365 nm) or (lower) visible light (>400 nm) irradiation for 10 min. Values represent the mean SD of the four separate experiments.

**Table 1**  
Cytotoxicity of the porphyrins against A549 cells in vitro

Compound	Cytotoxicity (IC <sub>50</sub> , μM)	
Porphyrin	UV	Visible
H <sub>2</sub> TPP	>20	>20
<b>6</b>	>20	>20
<b>7</b>	0.17	0.18
<b>8</b>	0.16	0.06
TMPyP	1.24	0.30

Tetraphenylporphyrin(H<sub>2</sub>TPP); tetra(4-N-methylpyridyl)porphyrin(TMPyP).

that of TMPyP is 0.30 μM. Similar results were also displayed in presence of UV light showing porphyrin **8** has shown higher phototoxicity (IC<sub>50</sub> = 0.16 μM) than TMPyP (IC<sub>50</sub> = 1.24 μM). The cytotoxicity could be arising through localization of porphyrin–quinoxaline conjugate **8** either in the cell membrane or mitochondria.

In summary, we have synthesized novel porphyrin–quinoxaline conjugates **6**, **7** and **8** and characterized. Their interactions with ctDNA showed two distinct binding modes suggesting intercalation followed by self-stacking along the DNA surface. The photocytotoxicity of conjugate **8** (IC<sub>50</sub> = 0.06 μM) against A549 cancer cells showed fivefold more potency than the standard TMPyP (IC<sub>50</sub> = 0.30 μM), and thus leading to be a potential candidate in developing a potent photocytotoxic agent for PDT. Further structure–activity relationship studies of these conjugates are in progress.

### Acknowledgments

We are grateful to the Department of Science & Technology and University Grants Commission, New Delhi (under SAP) for the financial support. We are thankful to RSIF, Chandigarh and AIRF, JNU for the NMR and MALDI spectra. B.M. is thankful to CSIR, New Delhi for SRF (F. No. 09/719(0042) /2011.EMR-I).

### Supplementary data

Supplementary data (experimental procedures and spectral data) associated with this article can be found, in the online version, at <http://dx.doi.org/10.1016/j.bmcl.2013.03.126>.

### References and notes

- Brown, S. B.; Brown, E. A.; Walker, I. *Lancet* **2004**, *5*, 497.
- Pandey, R. K.; Zengh, G.; Kadish, K. M.; Smith, K. M.; Guillard, R. *The Porphyrin Handbook*; Academic Press: San Diego, 2000. p 157.
- Josefsen, L. V.; Boyle, R. W. *Met-Based Drugs* **2008**, *2008*, 1.
- Boyle, R.; Dolphin, D. *Photochem. Photobiol.* **1996**, *64*, 469.
- Anantha, N. V.; Azam, M.; Sheardy, R. D. *Biochemistry* **1998**, *37*, 2709.
- Mettath, S.; Munson, B. R.; Pandey, R. K. *Bioconjugate Chem.* **1999**, *10*, 94.
- Feng, Q.; Nan-Qiang, L.; Yu-Yang, J. *Talanta* **1998**, *45*, 787.
- Feng, Q.; Nan-Qiang, L.; Yu-Yang, J. *Anal. Chim. Acta.* **1997**, *344*, 97.
- Hudson, B. P.; Sou, J.; Berger, D. J.; McMillin, D. R. *J. Am. Chem. Soc.* **1992**, *114*, 8997.
- Mestre, B.; Jakobs, A.; Pratviel, G.; Meunier, B. *Biochemistry* **1996**, *35*, 9140.
- Wilson, W. D.; Lynda, R.; Zhao, M.; Lucjan, S.; Boykin, D. *Biochemistry* **1993**, *32*, 4098.
- Ishikawa, Y.; Yamashita, A.; Uno, T. *Chem. Pharm. Bull.* **2001**, *49*, 287.
- Guo, C. C.; Li, H. P.; Zhang, X. B. *Bioorg. Med. Chem.* **2003**, *11*, 1745.
- Sehgal, I.; Sibrian-Vazquez, M.; Graca, M.; Vicente, H. *J. Med. Chem.* **2008**, *51*, 6014.
- Kumar, D.; Mishra, B.; Chandrashekar, K. P.; Kumar, A.; Akamatsu, K.; Kusaka, E.; Ito, T. *Chem. Commun.* **2013**, 683.
- Chaloin, L.; Bigey, P.; Loup, C.; Marin, M.; Galeotti, N.; Piechaczyk, M.; Heitz, F.; Meunier, B. *Bioconjugate Chem.* **2001**, *12*, 691.
- Bisland, S. K.; Singh, D.; Gariepy, J. *Bioconjugate Chem.* **1999**, *10*, 982.
- Sibrian-Vazquez, M.; Jensen, T. J.; Hammer, R. P.; Vicente, M. G. H. *J. Med. Chem.* **2006**, *49*, 1364.
- Gomer, C. J. *Photochem. Photobiol.* **1991**, *54*, 1093.
- Kim, Y. B.; Kim, Y. H.; Park, J. Y. *Bioorg. Med. Chem. Lett.* **2004**, *14*, 541.
- Sakata, G.; Makino, K.; Kurasawa, Y. *Heterocycles* **1998**, *27*, 2481.
- Kamal, A.; Azeza, S.; Malik, M. S.; Shaik, A. A.; Rao, M. V. *J. Pharm. Pharm. Sci.* **2008**, *11*, 56.
- (a) Toshima, K.; Takano, R.; Ozawa, T.; Matsumura, S. *Chem. Comm.* **2002**, 212; (b) Aggarwal, R.; Sumrana, G.; Kumar, V.; Mittal, A. *Eur. J. Med. Chem.* **2011**, *46*, 6083.
- Adler, A. D.; Longo, F. R.; Finarelli, J. D. *J. Org. Chem.* **1967**, *32*, 476.
- Kruper, W. J., Jr.; Chamberlin, T. A.; Kochanny, M. J. *Org. Chem.* **1989**, *54*, 2753.
- Harms, A. E. *Org. Process Res. Dev.* **2004**, *8*, 666.
- Spectral data of cationic porphyrin–quinoxaline conjugate 8*: <sup>1</sup>H NMR (400 MHz, DMSO-*d*<sub>6</sub>) δ: 9.58–9.55 (m, 6H), 9.16–9.03 (m, 8H), 8.99–8.87 (m, 6H), 8.75–8.72 (d, 2H *J* = 4 Hz), 8.48–8.44 (m, 7H), 8.42–8.40 (m, 1H), 4.84 (s, 9H), –2.98 (s, 2H). <sup>13</sup>C NMR (100 MHz, DMSO-*d*<sub>6</sub>) δ: 162.82, 151.66, 151.00, 148.08, 146.65, 145.37, 144.36, 144.13, 142.75, 138.68, 137.32, 133.16, 132.13, 131.89, 131.46, 131.01, 130.76, 130.37, 129.42, 127.76, 126.68, 120.65, 119.20, 116.97, 48.48. UV–vis λ<sub>max</sub> (nm): 422 (log ε = 5.1), 518 (log ε = 3.9), 582 (log ε = 3.7), 601 (log ε = 3.6), 656 (log ε = 3.3). IR (KBr) (ν<sub>max</sub> cm<sup>–1</sup>): 1138, 1402, 1483, 1514, 1643, 1687, 3010. MALDI-TOF *m/z*: calcd for C<sub>53</sub>H<sub>41</sub>N<sub>10</sub>O: 833.3448; Found: 833.3415 (M<sup>+</sup>). HPLC purity: 99.71%.
- (a) Carvlin, M.; Fiel, R. J. *Nucleic Acids Res.* **1983**, *11*, 6121; (b) McMillin, D. R.; McNett, K. M. *Chem. Rev.* **1998**, *98*, 1201; (c) Mohammadi, S.; Perree-Fauvet, M.; Gresh, N.; Hillairet, K.; Taillandier, E. *Biochemistry* **1998**, *37*, 6165; (d) Pasternack, R. F.; Gibbs, E. J.; Villafranca, J. J. *Biochemistry* **1983**, *22*, 2406.
- (a) Strickland, J. A.; Marzilli, L. G.; Wilson, W. D. *Biopolymers* **1990**, *29*, 1307; (b) Strahan, G. D.; Lu, D.; Tsuboi, M.; Nakamoto, K. J. *Phys. Chem.* **1992**, *96*, 6450.
- Pasternack, R. F.; Gibbs, E. J.; Gaudemer, A.; Antebi, A.; Bassner, S.; Poy, L. D.; Turner, D. H.; Williams, A.; Laplace, F.; Lansard, M. H.; Merienne, C.; Perree-Fauvet, M. *J. Am. Chem. Soc.* **1985**, *107*, 8179.
- Mukundan, N. E.; Petho, G.; Dixon, D. W.; Marzilli, L. G. *Inorg. Chem.* **1995**, *34*, 3677.
- Uno, T.; Hamasaki, K.; Tanigawa, M.; Shimabayashi, S. *Inorg. Chem.* **1997**, *36*, 1676.